

# MOBILE PANORAMIC MAPPING USING CCD-LINE CAMERA AND LASER SCANNER WITH INTEGRATED POSITION AND ORIENTATION SYSTEM

R. Reulke<sup>a,\*</sup>, A. Wehr<sup>b</sup>, D. Griesbach<sup>c</sup>

<sup>a</sup> Institute for Photogrammetry, University of Stuttgart - [Ralf.Reulke@ipho.uni-stuttgart.de](mailto:Ralf.Reulke@ipho.uni-stuttgart.de)

<sup>b</sup> Institute for Navigation, University of Stuttgart - [wehr@nav.uni-stuttgart.de](mailto:wehr@nav.uni-stuttgart.de)

<sup>c</sup> German Aerospace Center DLR, Competence center - [Denis.Griesbach@dlr.de](mailto:Denis.Griesbach@dlr.de)

**KEY WORDS:** Digital panoramic camera, laser scanner, data fusion, mobile mapping

## ABSTRACT:

The fusion of panoramic camera data with laser scanner data is a new approach and allows the combination of high-resolution image and depth data. Application areas are city modelling, virtual reality and documentation of the cultural heritage. Panoramic recording of image data is realized by a CCD-line, which is precisely rotated around the projection centre. In the case of other possible movements, the actual position of the projection centre and the view direction has to be measured. Linear moving panoramas e.g. along a wall are an interesting extension of such rotational panoramas. Here, the instantaneous position and orientation determination can be realized with an integrated navigation system comprising differential GPS and an inertial measurement unit.

This paper investigates the combination of a panoramic camera and a laser scanner with a navigation system for indoor and outdoor applications. First it will be reported about laboratory experiments, which were carried out to obtain valid parameters about the surveying accuracy achievable with both sensors panoramic camera and laser scanner respectively. Then out door surveying results using a position and orientation system as navigation sensor will be presented and discussed.

## 1. INTRODUCTION

Generation of city models offering a high realistic visualisation potential requires three-dimensional imaging sensors with high 3D resolution and high image quality. Today commonly used sensors offer either a high image quality or high depth accuracy. Therefore, the idea and the vision of a system were borne to integrate available independent measurement systems. For the acquisition of high resolution image and depth data from extended object, e.g. building facades, a high resolution camera for the image information, a laser scanner for the depth information and position and orientation system (POS) for georeferencing must be integrated.

High resolution images can be acquired by CCD-matrix and line sensors. Main advantage of line sensors is the generation of high resolution images without merging or stitching of images patches like in matrix imaging. A problem is an additional sensor motion of the CCD-line to achieve the second image dimension. An obvious solution is the accurate rotation around CCD-line axis on a turn table as used in panoramic imaging.

The depth image or the surfaces of the imaged area can be acquired very precisely in a reasonable short time with laser scanners. However, these systems very often sample only depth data with poor horizontal resolution. Some of them offer monochrome intensity images of poor quality in the spectral range of the laser beam (e.g. NIR). Very few commercial laser scanners use additional imaging colour sensors for obtaining coloured 3D images.

However, with regard to building surveying and setting up cultural heritage archives the imaging resolution of laser scanner data must be improved. This can be achieved by combining data from a high-resolution digital 360° panoramic camera with data from a laser scanner. Fusing these image data with 3D information of laser scanning surveys very precise 3D models with detailed texture information will be obtained. This approach is related to 360° geometry.

Large linear structures like city facades can be acquired with panoramic approach only from different standpoints with variable resolution of the object. To overcome this problem, laser-scanner and panoramic camera should be linear moved along e.g. a building facade. Applying this technique the main problem is georeferencing and fusing the two data sets of the panoramic camera and the laser scanner respectively. An additional accurate attitude measurement is necessary for each measured CCD- and laser-line.

The experimental results shown in the following will deal with this problem and will lead to an optimum surveying setup comprising a panoramic camera, laser scanner and a POS. This surveying and documentation system will be called POSLAS-PANCAM (POS supported laser scanner panoramic camera).

To verify these approach first experiments were carried out in the laboratory and in the field with the Digital 360° panoramic camera (M1), the 3D-Laserscanner (3D-LS) and a Position and Orientation System (POS).

The objectives of the experiments are to verify the concepts and to obtain design parameters for a compact and handy system for combined data acquisition and inspection.

## 2. SYSTEM

The measurement system consists of a combination of an imaging system, a laser scanner and a system for attitude determination.

### 2.1 Digital 360° Panoramic Camera (M2)

The digital panoramic camera EYESCAN will be preliminary used as a measurement system to create high-resolution 360° panoramic images for photogrammetry and computer vision (Scheibe, 2001, Klette, 2001). The sensor principle is based on a CCD line, which is mounted on a turntable parallel to the rotation direction. Moving the turntable generates the second

---

\* Corresponding author

image direction. To reach highest resolution and a large field of view a CCD-line with more than 10,000 pixels is used. This CCD is a RGB triplet and allows acquiring true colour images. A high SNR electronic design allows a short capture time for a 360° scan.

EYESCAN is designed for rugged everyday field use as well as for the laboratory measurement. Combined with a robust and powerful portable PC it becomes easy to capture seamless digital panoramic pictures. The sensor system consists of the camera head, the optical part (optics, depth dependencies) and the high precision turntable with DC-gear-system motor.

Number of Pixel	3*10200 (RGB)
Radiometric dynamic/resolution	14 bit / 8 bit per channel
Shutter speed	4ms up to infinite
Data rate	15 Mbytes / s
Data volume 360° (optics f=60mm)	3GBytes
Acquisition time	4 min
Power supply	12 V

Table 1. Technical parameter of the digital panoramic camera

Table 1 summarise the principle features of the camera: The camera head is connected to the PC with a bidirectional fibre link for data transmission and camera control. The camera head is mounted on a tilt unit for vertical tilt of ±30° with 15° stops. Axis of tilt and rotation are in the needlepoint.

The pre-processing of the data consists of data correction (PRNU, DSNU, offsets) and a (non linear) radiometric normalisation to cast the data from 16 to 8 bit. All this procedures can be run in real time or off line. Additional software parts are responsible for real-time visualisation of image data, a fast preview for scene selection and a quick look during data recording.

## 2.2 The Laser Scanner 3D-LS

In the experiments M2 images were supported by the 3D-LS depth data. This imaging laser scanner carries out the depth measurement by side-tone ranging (Wehr, 1999). This means, the optical signal emitted from a semiconductor laser is modulated by high frequency signals. As the laser emits light continuously such laser system are called continuous wave (cw) laser system. The phase difference between the transmitted and received signal is proportional to the two-way slant range. Using high modulation frequencies, e.g. 314 MHz, resolutions down to the tenth of a millimetre are possible.

Besides depth information these scanners sample for each measurement point the backscattered laser light with a 13 bit resolution. Therefore, the user obtains 3D surface images. The functioning of the laser scanner is explained in (Wehr, 1999). The technical parameter are compiled in Table 2

Laser power	0.5 mW
Optical wavelength	670 nm
Inst. field of view (IFOV)	0.1°
Field of view (FOV)	30° x 30°
Scanning pattern	- 2-dimensional line (standard) - vertical line scan - free programmable pattern

Pixels per image	max. 32768 x 32768 pixels
Range	< 10 m
Ranging accuracy	0.1 mm (for diffuse reflecting targets, ρ=60%, 1 m distance)
Measurement rate	2 kHz (using on side tone) 600 Hz (using two side tones)

Table 2. Technical parameter of 3D-LS

## 2.3 Applanix POS-AV 510

The attitude measurement is the key problem of this combined approach. For demonstration we use the airborne attitude measurement system POS AV 510 from Applanix, which is designed for those applications that require both excellent absolute accuracy and relative accuracy. An example of this would be a high altitude, high resolution digital line scanner.

The absolute measurement accuracy after post processing is 5-30 cm in position,  $\delta\theta=\delta\phi=0.005^\circ$  for pitch or roll and  $\delta\psi=0.008^\circ$  for heading.

For an object distance D the angle dependent spatial accuracy d is therefore

$$d = D \cdot \delta \quad (\delta \text{ in rad}).$$

For an object distance D=10m the spatial accuracy is  $d \approx 1\text{mm}$  and appropriate for verification of a mobile mapping application.

For a future mobile mapping system a simpler attitude measurement, which is also less expensive is necessary. For this purpose we expect in the next few years new gyro development and improved post processing algorithms.

## 2.4 POSLAS-PANCAM

Figure 1 shows the mechanical integration of the three sensor systems. In the following POSLAS-PANCAM will be abbreviated to PLP-CAM. This construction allows a precise relation between 3D-LS and panoramic data which is the main requirement for data fusion. The 3D-LS data are related to the POS data as the lever arms were minimised with regard to the laser scanner and are well defined by the construction.



Figure 1. PLP-CAM

The different items of PLP-CAM have to be synchronized exactly, because each system works independently. The block chart in Figure 2 shows the approach. Using event markers solves the problem by generating time stamps. These markers are stored by POS and combine a measurement event with absolute GPS-time (e.g. starting a scanning line).

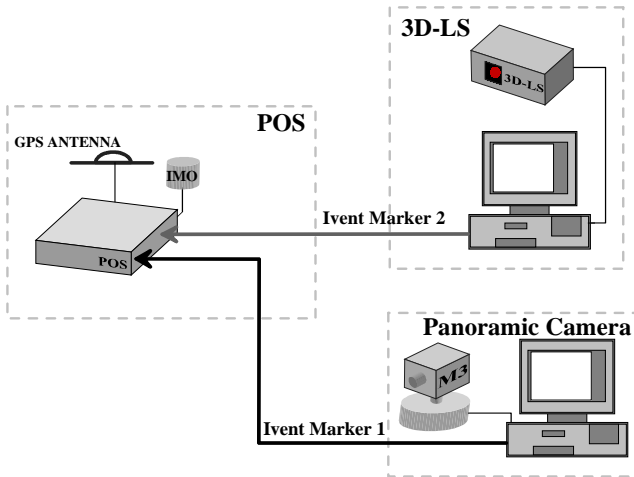


Figure 2. Synchronization

### 3. FUSION OF M1 AND 3D-LS DATA

To investigate the fusion of panoramic and laser data first experiments were carry out in a laboratory environment. Here, only the panoramic camera M2 and 3D-LS were used.

#### 3.1 Experimental Set-up

In order to study the problems arising by fusion of data sets of the panoramic camera and the 3D-LS, both instruments took an image of a special prepared scene, which were covered with well-defined control points. The panoramic camera was mounted on a tripod. After recording completion the camera was dismantled and 3D-LS were mounted on the tripod without changing the tripod's position. 3D-LS were used in the imaging mode scanning a field of view (FOV) of  $40^\circ \times 26^\circ$  comprising  $1600 \times 1000$  pixels. Each pixel is described by the quadruple Cartesian coordinates plus intensity  $(x, y, z, I)$ . The M2-image covered a FOV of approximately  $30^\circ \times 60^\circ$  with  $5000 \times 10000$  pixels.



Figure 3. Special prepared laboratory

66 control points were available in a distance of 6 m. Lateral resolution of laser and panoramic scanner is 3 mm and 1.05 mm respectively, which is a suitable value for fusion of the data sets. For the coordinate determination of the signalled points an independent approach was done. Using image data from a DCS 460 camera and bundle block adjustment program Australis. The lateral accuracy of about 30 points is 0.5 mm and depth accuracy about 3 mm.



Figure 4. PANCAM on tripod

#### 3.2 Modelling and Calibration

Laser scanner and panoramic camera work with different coordinate systems and must be adjust one to each other. The laser scanner delivers Cartesian coordinates; where as M2 puts out data in a typical photo image projection. Although, both devices were mounted at the same position one had to regard that the projection centre of both instruments were not located exactly in the same position. Therefore a model of panoramic imaging and a calibration with known target data is required.

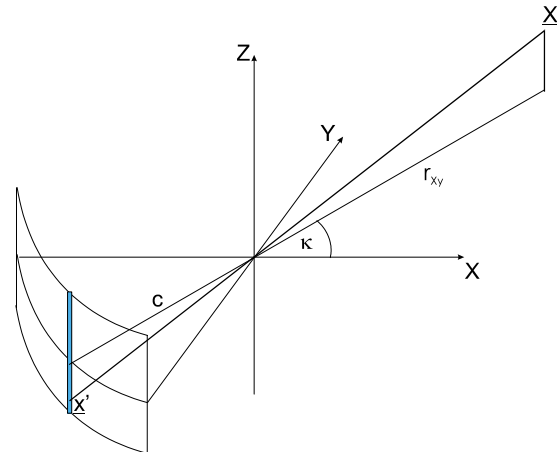


Figure 4. Panoramic imaging (see text)

The imaging geometry of the panoramic camera is characterized by the rotating CCD-line, assembled perpendicular to the  $x$ - $y$  plane and forming an image by rotation around the  $z$ -axis. The modelling and calibration of panoramic cameras was investigated and published recently (Schneider, 2002 & 2003, Klette, 2001 & 2003).

For camera description and calibration we use the approach shown in Figure 4. The CCD-line is placed in the focal plate perpendicular to the  $z'$ -axis and shifted with respect to the  $y'$ - $z'$  coordinate origin by  $(y'_0, z'_0)$ . The focal plate is mounted in the camera at a distance  $x'$ , which is suitable to the object geometry. If the object is far from the camera the CCD is placed in the focal plane of the optics at  $x'=c$  (the focal length) on the  $x'$ -axis behind the optics (lower left coordinate system). To form an image, the camera is rotated around the origin of a  $(x, y)$  coordinate system.

To derive the relation between object point  $X$  and a pixel in an image the colinearity equation can be applied.

$$\underline{X} - \underline{X}_0 = \lambda \cdot (\underline{x} - \underline{x}_0) \quad (1)$$

$\underline{x}$  is the image coordinate,  $\underline{X}_0$  and  $\underline{x}_0$  are the projection centre for the object and the image space. To see this object point with a pixel of the CCD-line on the focal plate, the camera has to be rotated by an angle of  $\kappa$  around z-axis. For the simplest case ( $y_0=0$ ) the result is

$$(\underline{X} - \underline{X}_0) = \lambda \cdot \underline{R}^T \cdot (\underline{x}' - \underline{x}'_0) = \lambda \cdot \begin{bmatrix} \cos \kappa & -\sin \kappa & 0 \\ \sin \kappa & \cos \kappa & 0 \\ 0 & 0 & 1 \end{bmatrix} \cdot \begin{bmatrix} -c \\ 0 \\ z' - z'_0 \end{bmatrix} = \lambda \cdot \begin{bmatrix} -c \cdot \cos \kappa \\ -c \cdot \sin \kappa \\ z' - z'_0 \end{bmatrix} \quad (2)$$

To derive some important parameters of the camera, a simplified approach is used. The unknown scale factor can be calculated from the square of the x-y components of this equation:

$$\lambda = \frac{r_{XY}}{c} \quad r_{XY} = \sqrt{(X - X_0)^2 + (Y - Y_0)^2} \quad (3)$$

The meaning of  $r_{XY}$  can easily be seen in Figure 4. This result is a consequence of the rotational symmetry. By dividing the first two equations and using the scale factor for the third, the following equations deliver an obvious result, which can be geometrically derived from Figure 4.

$$\frac{\Delta Y}{\Delta X} = \tan \kappa \quad \text{and} \quad \Delta Z = r_{XY} \cdot \frac{\Delta Z'}{c} \quad (4)$$

The image or pixel coordinates ( $i, j$ ) are related to the angle  $\kappa$  and the z-value. Because of the limited image field for this investigation, only linear effects (with respect to the rotation and image distortions) should be taken into account:

$$i = \frac{1}{\delta \kappa} \cdot a \tan \frac{\Delta Y}{\Delta X} + i_0 \quad j = \frac{c}{\delta z} \cdot \frac{\Delta Z}{r_{XY}} + j_0 \quad (5)$$

$\delta z$  pixel distance  
 $\delta \kappa$  angle of one rotation step  
 $c$  focal length

The unknown or not exactly known parameters  $\delta \kappa$ ,  $i_0$ ,  $c$  and  $j_0$  can be derived from known marks in the image field.

For calibration we used signalized points randomly distributed and in different distances from the camera. The analyzing of the resulting errors in the object space shows, that the approach (4) and (5) must be extended. Following effects should be incorporated:

- Rotation of the CCD (around x-axis)
- Tilt of the camera (rotation around y-axis)

This effect can be incorporated into equation (2). The variation of the angel  $\varphi$  and  $\omega$  should be small ( $\sin \varphi = j$ ,  $\cos \varphi = 1$  and  $\sin \omega = \omega$ ,  $\cos \omega = 1$ )

$$(\underline{x}' - \underline{x}'_0) = \lambda^{-1} \cdot \underline{R} \cdot (\underline{X} - \underline{X}_0) = \lambda \cdot \begin{bmatrix} \cos \kappa & \sin \kappa & \omega \cdot \sin \kappa - \varphi \cdot \cos \kappa \\ -\sin \kappa & \cos \kappa & \omega \cdot \sin \kappa + \varphi \cdot \sin \kappa \\ \varphi & -\omega & 1 \end{bmatrix} \cdot \begin{bmatrix} X - X_0 \\ Y - Y_0 \\ Z - Z_0 \end{bmatrix} \quad (6)$$

For this special application the projection centre of the camera is  $(X_0, Y_0, Z_0) \equiv (0, 0, 0)$ . With a spatial resection approach, based on equation (6), the unknown parameter of exterior orientation can be derived.

Despite the limited number of signalized points and the small field of view of the scene ( $30^\circ \times 30^\circ$ ) the accuracy of the panorama camera model is  $\sigma \approx 3$  image pixel of the camera. Using an improved model and the program from Schneider TU-Dresden an accuracy of better than one pixel can be achieved.

### 3.3 Fusion of Panoramic and Laser Scanner Data

Before the data of M2 and 3D-LS can be fused, the calibration of the 3D-LS must be checked. The test field shown in figure 4 was used for this purpose. 3D-LS deliver 3D point clouds. The mean distance between points is about 2-3 mm at the wall. As the depth and image data do not fit to a regular grid they cannot be compared with rasterised image data of a photogrammetric survey without additional processing.

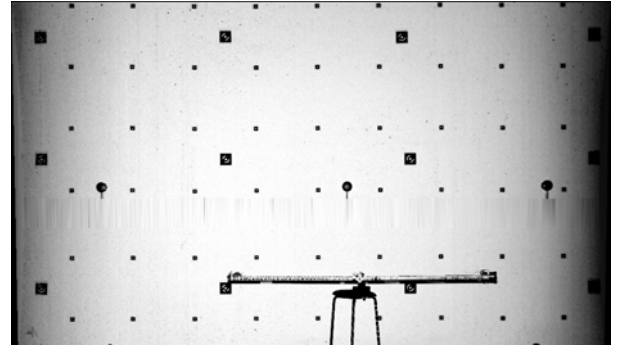


Figure 5. Laser image data

First the 3D-LS data are triangulated and then the rasterized data is computed by interpolation on a regular grid (s. Figure 5). This procedure was carried out by the program ENVI. Now, 3D-LS data can be compared with data from a matrix camera. Applying a bundle block adjustment on the image data of the matrix camera delivers the interior orientation and the absolute coordinate system is built up by an additional 2 m reference. In order to compare object data the following coordinate transform is required:

$$\begin{pmatrix} X_i \\ Y_i \\ Z_i \end{pmatrix} = \begin{pmatrix} X_0 \\ Y_0 \\ Z_0 \end{pmatrix} + \begin{pmatrix} r_{11} & r_{12} & r_{13} \\ r_{21} & r_{22} & r_{23} \\ r_{31} & r_{32} & r_{33} \end{pmatrix} \cdot \begin{pmatrix} x_i \\ y_i \\ z_i \end{pmatrix} \quad (6)$$

$\underline{x}_i$  are the points in the laser coordinate system and  $\underline{X}_i$  in the camera system.  $\underline{X}_0$  and  $r_{ij}$  are the unknown transform parameter, which can be derived by a least square fit. After the transform the accuracy for the 3D-LS can be determined in horizontal direction to 0.5 mm or  $\frac{1}{4}$  pixel and in vertical direction to 1 mm or  $\frac{1}{2}$  pixel, if the photogrammetric survey is regarded as a reference. A tendency for outliers cannot be observed.

In a further processing step laser data and panoramic data can be merged. As both data sets are in different coordinate systems first a transformation between both coordinate systems must be determined by using reference points. The calibration procedure, as shown in chapter 3.2 delivers a relation between image coordinates ( $i, j$ ) and object points ( $X, Y, Z$ ). Now, all 3D-LS distance data can be transformed in the panoramic coordinate system and by that its pixel position in the panoramic image can be computed. For this position the actual grey value of the panoramic camera is correlated to the instantaneous laser image point. Figure 6 depicts the combination of both images. The ground sampling at the wall is about 1.5 mm. The fact that colour shifts are not visible in the

image verifies the calculated alignment between both systems. The strong red shift is caused by the black cable carrying board (s. Figure 3). This board causes poor 3D laser scanner data due to bad reflecting properties.

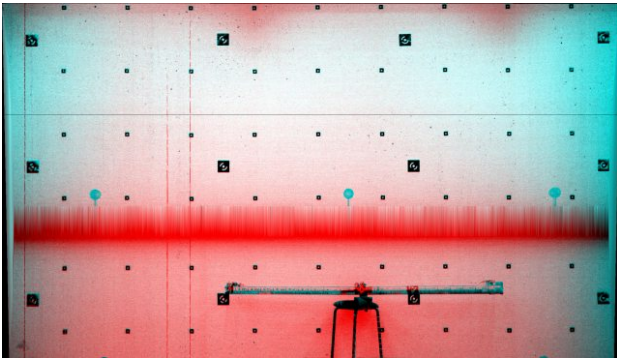


Figure 6. Merged images of 3D-LS and Panoramic Camera

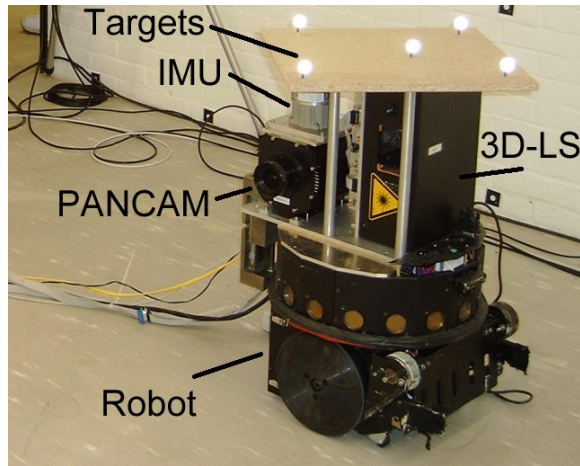


Figure 7. PLP-CAM carried by robot

#### 4. POSLAS-PANCAM

Before the POSLAS-PANCAM was used in field experiment the recording principle was studied in a laboratory environment.

##### 4.1 POSLAS-PANCAM in Laboratory

The functioning of POSLAS-PANCAM (PLP-CAM) was first verified by surveying the test field described in chapter 3. During this experiment a robot was used as a moving platform. As GPS reception was impossible in the laboratory the position data and orientation data were obtained from the camera tracking system ARTTrack2 which comprises two CCD cameras. The IMU measurement data were also recorded parallel. This means, redundant orientation information is available and the accuracy of the orientation system can be verified. Figure 7 shows the robot with PLP-CAM. Figure 8 depicts one of the two tracking cameras. The robot is remotely controlled by a joystick.



Figure 8. PLP-CAM robot and tracking camera

The results of these experiments were used to develop algorithms to integrate the data of the three independently working systems. It could be shown, that the data sets can be well synchronized. Furthermore, the whole system could be calibrated by using the targets (s. Figure 3).

##### 4.1 POSLAS-PANCAM in the Field

For a field experiment the PLP-CAM was mounted in a surveying van. The GPS-antenna of POS was installed on top of the vehicle. The car drove along the facade of the Neues Schloss in Stuttgart (s. Figure 9).



Figure 9. PLP-CAM in front of Neues Schloss Stuttgart

As the range performance of the 3D-LS was too low, only image data of the CCD-line camera and the POS-Data were recorded. The left image in Figure 10 shows the rectification result on the basis of POS data alone. By applying image processing algorithms the oscillation can be reduced and a comprehensive correction is achieved by using external laser scanner data recorded independently during another survey (s. right image in Figure 10).

The high performance of the line scan camera is documented in Figure 11 and Figure 12. A heraldic animal at Schloss Solitude in Stuttgart was surveyed by PLP-Cam. The object is hardly recognizable (s. Figure 12) from the original PANCAM data. However, after correcting the data a high quality image is obtained. The zoomed in part illustrates the high camera performance.

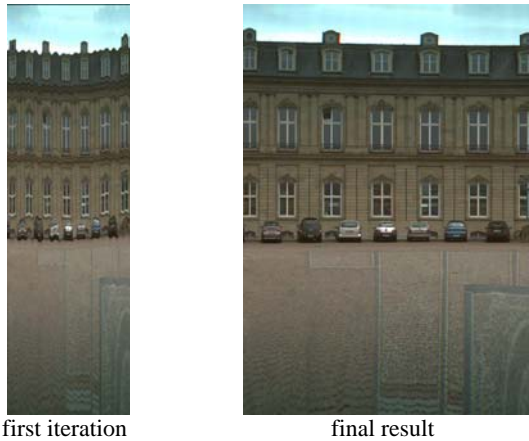


Figure 10. Survey with PLP-CAM

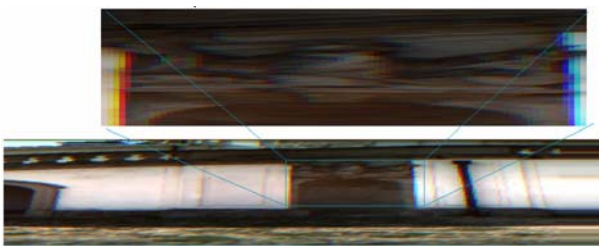


Figure 11. Original scanned data with panoramic camera



Figure 12. Result after correction

## 5. CONCLUSIONS

The experiments fusing M3 data with 3D-LS data show that using such an integrated system high resolved 3D-images can be computed. The processing of the two independent data sets makes clear that a well defined and robust assembly is required, because it benefits from the well defined locations of the different origins and the relative orientation of the different devices with respect to each other. The system can be calibrated very precisely by using a sophisticated calibration field equipped with targets which could be identified and located very accurately with both PANCAM and 3D-LS. The field experiments with PLP-CAM demonstrated that in courtyards and in narrow street with high buildings one has to face poor GPS signals. Here, the POS-AV system of Applanix company

worked very degraded, because it is designed for airborne applications, where one do not have to regard obscurations and multipath effects. For this application POS-LV system of Applanix will deliver improved results. For all that the presented examples make clear that very detailed illustrations of facades including 3D-information can be obtained by fusing POS, M3 and 3D-LS data.

## REFERENCES:

Klette, R.; Gimelfarb, G.; Reulke, R., 2001. Wide-Angle Image Acquisition, Analysis and Visualization, Vision Interface 2001, Proceedings, pp. 114-125.

Klette, R.; Gimelfarb, G.; Huang, F.; Wei, S. K.; Scheele, M.; Scheibe, K.; Börner, A.; Reulke, R. 2003. A Review on Research and Applications of Cylindrical Panoramas, CITR-TR-123

Reulke, R.; Scheele, M.; Scheibe, K. u.a., 2001. Multi-Sensor-Ansätze in der Nahbereichsphotogrammetrie, 21. Jahrestagung DGPF, Konstanz, Sept. 2001, DGPF, Photogrammetrie und Fernerkundung.

Scheele, M., Börner, A., Reulke, R., Scheibe, K., 2001. Geometrische Korrekturen: Vom Flugzeugscanner zur Nahbereichskamera; Photogrammetrie, Fernerkundung, Geo-information.

Scheibe, K., Korsitzky, H., Reulke, R., Scheele, M., Solbrig, M., 2001. EYESCAN – A high resolution digital panoramic camera, LNCS 1998, Springer, Berlin 2001, pp. 77.

Schneider, D., Maas, H.-G., Geometrische Modellierung und Kalibrierung einer hochauflösenden digitalen Rotationszeilenkamera, DGPF-Tagung, 2002

Schneider, D., 2003. Geometrische Modellierung und Kalibrierung einer hochauflösenden digitalen Rotationszeilenkamera, 2. Oldenburger 3D-Tage, 27.2.

Wehr, A., 1999. 3D-Imaging Laser Scanner for Close Range Metrology. Proc. of SPIE, Orlando, Florida, 6-9 April 1999, Vol. 3707: pp. 381-389.

Australis home page

<http://www.sli.unimelb.edu.au/australis/index.htm>

## Acknowledgements:

The authors would like to thank Prof. P. Levi Institute of Parallel and Distributed Systems, University of Stuttgart for making available the robot, Prof. H.-G. Maas and D. Schneider Institute of Photogrammetry and Remote Sensing TU-Dresden for processing PLP-CAM data, Dr. M. Schneberger Advanced Realtime Tracking GmbH, Herrsching making available the camera tracking system ARTTrack2 and Mr. M. Thomas Institute of Navigation University Stuttgart for his outstanding support during the laboratory and field experiments and in processing the laser data and realizing the synchronization.